

# Grey correlation analysis between strength of slag cement and particle fractions of slag powder

Yongjuan Zhang <sup>\*</sup>, Xiong Zhang

*Building Material Institute, Tongji University, 1239 Siping Road, Shanghai 200092, China*

Received 21 February 2006; received in revised form 29 October 2006; accepted 16 February 2007

Available online 2 March 2007

## Abstract

The particle size distributions of slag powder were investigated by Laser Scatter equipment. The influence of particle fractions of slag powder on the compressive strength of slag cement composed of 50% slag powder and 50% Portland cement was also studied by the method of grey correlation analysis. The results indicated that the volume fraction of particles 5–10  $\mu\text{m}$  had a maximum positive effect on the mortar compressive strength of slag cement at 7 d and the volume fraction of particles 10–20  $\mu\text{m}$  had a maximum positive effect on the mortar compressive strength at 28 d, whereas the volume fraction of particles larger than 20  $\mu\text{m}$  had a negative effect on the mortar compressive strength at 7 and 28 d.

© 2007 Elsevier Ltd. All rights reserved.

*Keywords:* Slag powder; Particle fraction; Mortar compressive strength; Grey correlation analysis

## 1. Introduction

Fly ash, slag powder and silica fume are effective admixtures used in various types of high performance concrete (HPC) [1–4]. The HPC made by Li and Yao [5] has a compressive strength of 100 MPa, which is related with specific area of admixture intimately. In fact, the activity of slag powder indicated only by specific area is not suitable. The particle size distribution of admixture powder has also a great effect on its activity.

Many studies have been done to examine the relationships between cement particle size distribution and the hydration kinetics and hardened paste strength properties [6–11]. For a given water-to-cement ratio, a reduction in median particle size generally results in an increased hydration rate and, therefore, improved early properties such as high early strength. For this reason, the fineness of Portland cement has been generally increased over the years. Bentz et al. [12] explored the effect of cement particle size distribution on a variety of performance properties via

computer simulation and a few experimental studies. Some investigators have studied the relationship between the particle size distribution of admixture powder and its properties, too. Ranganath et al. [13] examined the role of different size fraction of pounded ash on the lime-reactivity strength of ash-lime-sand mortar by classifying pounded ash into three different size fractions. Olorunsogo [14] reported an investigation into the influence of particle size distribution of ground granulated blast furnace slag with different PSDs (as represented by the parameters of the Rosin–Rammler distribution function) on the bleeding characteristics of slag cement mortar. Grzeszczyk and Lipowski [15] investigated the effect of content and particle size distribution of high-calcium fly ash on the rheological properties of cement pastes. Mehta [16] has studied the particle size distribution of low calcium fly ash. The results indicated that the activity of fly ash and the volume fraction of particles had a positive relationship when particles were less than 10  $\mu\text{m}$  and had a negative relationship when particles were larger than 45  $\mu\text{m}$ . In this paper, a slag sample from steel factory was used to study the relationship between the activity of slag cement and particle fractions of slag. The slag sample was ground into different particle

<sup>\*</sup> Corresponding author. Tel.: +86 659 83465; fax: +86 21 659 80530.  
E-mail address: [zyj1960@21cn.com](mailto:zyj1960@21cn.com) (Y. Zhang).

size distributions. Some slag cement samples made from slag powder and Portland cement were prepared and the relationship between the mortar compressive strength and slag powder fraction was studied by grey correlation analysis. The research on the micro-analysis of the slag cement pastes proved the macro test and grey correlation analysis. The purpose of the study is to differentiate which fraction of slag powder is favorable to slag cement and which fraction of slag powder is disadvantageous to slag cement. That will help us to develop improved slag cement from slag powder and Portland cement by adjusting the particle size distribution of slag powder.

**2. The principle of the grey correlation analysis**

The principle of the grey correlation analysis [17,18] is based on the macro or micro geometric approachment between the behavior factors. The more similar are the array curves, the closer connection they have. Fig. 1 is a statistics graph of agriculture production in a certain district in China. From the figure we can see that the most similar curve with the total agriculture production value (called main-array or main-factor) is the total planting production value (called sub-array or sub-factor). Therefore, the planting production is essential for the agriculture production in that district and stock raising, forest and fruit production are minor. The detailed calculation formulas are as follows.

The arrays are as follows:

$$\begin{aligned} &\{X_0^{(0)}(r)\}, \quad r = 1, 2, 3, \dots, N_0 \\ &\{X_1^{(0)}(r)\}, \quad r = 1, 2, 3, \dots, N_1 \\ &\{X_2^{(0)}(r)\}, \quad r = 1, 2, 3, \dots, N_2 \\ &\dots \\ &\{X_k^{(0)}(r)\}, \quad r = 1, 2, 3, \dots, N_k \end{aligned}$$

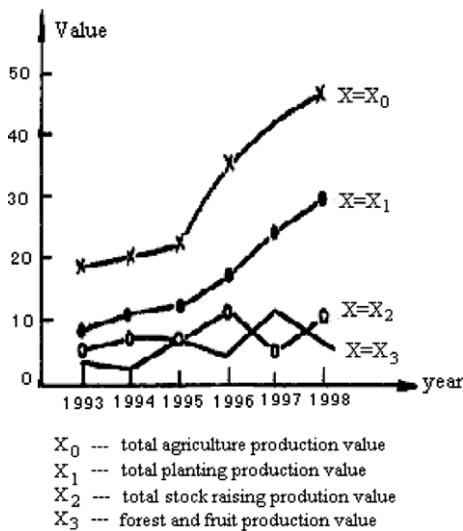


Fig. 1. Statistics of agriculture production in a certain district in China from 1993 to 1998.

Among them,  $N_1, N_2, \dots, N_k$  belong to natural number and they may be not equal. The  $k$  arrays express  $k$  factors. The array  $\{X_0^{(0)}(r)\}$  is assigned to main-array and  $\{X_m^{(0)}(r)\}$  ( $m = 1, 2, \dots, k$ ) to sub-arrays.

The average of  $\{X_m^{(0)}(r)\}$ ,  $r = 1, 2, 3, \dots, N_m$ ,  $m = 0, 1, 2, \dots, k$  is  $\bar{X}_m$

$$\bar{X}_m = \frac{1}{N_m} \left[ \sum_{r=1}^{N_m} X_m^{(0)}(r) \right]$$

The conversion  $Y_m(r) = X_m^{(0)}(r)/\bar{X}_m$  is made and then following arrays called inverted arrays can be obtained:

$$\begin{aligned} &\{Y_0(r)\}, \quad r = 1, 2, 3, \dots, N_0 \\ &\{Y_1(r)\}, \quad r = 1, 2, 3, \dots, N_1 \\ &\{Y_2(r)\}, \quad r = 1, 2, 3, \dots, N_2 \\ &\dots \\ &\{Y_k(r)\}, \quad r = 1, 2, 3, \dots, N_k \end{aligned}$$

In fact, the transformation from  $\{X_m^{(0)}(r)\}$  into  $\{Y_m(r)\}$  can be regarded as a reflection.

Table 1  
Chemical compositions of raw materials

Material	Si <sub>2</sub> O <sub>3</sub>	Fe <sub>2</sub> O <sub>3</sub>	Al <sub>2</sub> O <sub>3</sub>	CaO	MgO	f-CaO
Clinker	20.66	5.18	6.03	64.7	1.21	0.67
Gypsum	5.97	0.43	1.78	30.34	1.26	–
Slag	33.18	1.53	13.19	39.25	9.36	–

Table 2  
The LS results of slag powder

Particle size (μm)	Sample					
	Sa	Sb	Sc	Sd	Se	Sf
<i>Undersize product, V (%)</i>						
1	2.54	6.33	7.69	3.93	7.32	8.92
2	6.11	10.7	18.1	8.23	14.0	18.3
3	9.27	15.7	28.1	12.3	21.2	28.9
4	12.2	21.4	36.6	16.1	28.3	38.6
5	15.0	27.3	43.5	19.5	35.1	46.8
6	17.7	33.1	49.3	22.7	41.3	53.3
8	22.7	43.3	58.4	28.3	51.4	62.8
10	27.3	51.7	65.2	32.9	58.9	69.0
15	37.2	66.2	76.7	41.7	70.6	77.6
20	45.5	75.9	84.8	48.9	78.3	83.5
25	52.7	83.2	90.3	55.2	83.9	87.8
30	58.8	88.4	93.6	60.5	87.8	90.6
40	68.6	94.5	96.9	69.3	92.5	94.3
50	76.1	97.4	98.3	76.0	94.9	96.3
60	82.0	98.8	99.0	80.9	96.4	97.4
80	90.2	99.8	99.5	86.8	97.8	98.8
90	92.9	99.96	99.7	88.7	98.2	99.1
100	94.8	99.99	99.7	90.2	98.4	99.3
150	98.6	100	99.9	94.3	99.5	99.6
200	99.3	100	100	96.0	99.7	99.7
Average diameter (μm)	35.45	16.61	10.98	33.98	12.26	10.43
Blaine fineness (m <sup>2</sup> /kg)	233	405	533	256	493	563

The absolute difference  $\Delta_{om}(r)$  between  $\{Y_m(r)\}$  and  $\{Y_0(r)\}$  at  $t = r$  is:

$$\Delta_{om}(r) = |Y_0(r) - Y_m(r)|, \quad r = 1, 2, 3, \dots$$

The minimum value and the maximum value among  $\Delta_{om}(r)$  can be found out and named as  $\Delta_{0m}(\min)$  and  $\Delta_{0m}(\max)$ , and then the minimum value (expressed as  $\Delta(\min)$ ) and the maximum value (expressed as  $\Delta(\max)$ ) among all the values of  $\Delta_{0m}(\min)$  and  $\Delta_{0m}(\max)$  can be found out, too. The grey correlation coefficient  $\xi_{om}(r)$  at  $t = r$  is

$$\xi_{om}(r) = [\Delta(\min) + K\Delta(\max)] / [\Delta_{om}(r) + K\Delta(\max)]$$

$K$  is recognition coefficient in the formula and defined as 0.5.

The grey correlation degree of  $Y_m$  and  $Y_0$  is:

$$\zeta_{om} = \left[ \sum_{r=1}^N \xi_{om}(r) \right] / N$$

Because  $\Delta_{om}(r) = |Y_0(r) - Y_m(r)|$  is used, the grey correlation polarity between factors cannot be separated. The formulas below are used to judge it:

$$Q_m = \sum_{r=1}^N rY_m(r) - \sum_{r=1}^N Y_m(r) \sum_{r=1}^N r/N$$

$$Q_r = \sum_{r=1}^N r^2 - \left( \sum_{r=1}^N r \right)^2 / N.$$

When  $\text{sign}(Q_m/Q_r) = \text{sign}(Q_o/Q_r)$ ,  $Y_m$  and  $Y_0$  are positive correlation. When  $\text{sign}(Q_m/Q_r) = -\text{sign}(Q_o/Q_r)$ ,  $Y_m$  and  $Y_0$  are negative correlation.

The grey correlation degree is a quantitative value of the correlation between the factors. If the value of grey correlation degree is higher, the main-factor and sub-factor are more relevant. Positive correlation between main-array and sub-array indicates that the sub-factor will enhance the main-factor. However, negative correlation between main-array and sub-array indicates that the sub-factor will weaken the main-factor.

Table 3  
The mortar compressive strength of slag cement (MPa)

Age	Sample					
	CSa	CSb	CSc	CSd	CSe	CSf
7 d	26.6	35.3	41.0	35.3	42.9	45.8
28 d	56.2	70.2	57.8	63.0	67.2	63.7

Table 4  
The LS results of slag powder X and C

Sample	Particle size ( $\mu\text{m}$ )							
	5	10	15	20	30	40	50	60
<i>Undersize product, V (%)</i>								
X	28.9	56.7	78.1	95.2	100	100	100	100
C	0	0	1.16	6.04	30.5	48.9	59.7	71.8

### 3. Experimental procedure

#### 3.1. Material

Blast furnace slag, clinker and gypsum were obtained from the cement factory. Table 1 shows the chemical com-

Table 5  
The mortar compressive strength of special slag cement (MPa)

Age	Sample	
	TX	TC
7 d	47.8	21.2
28 d	69.7	46.3

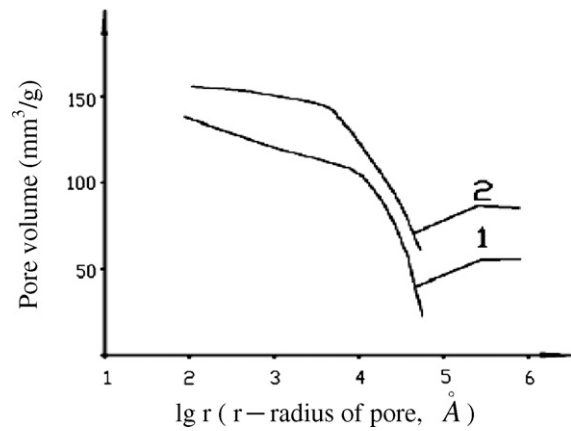


Fig. 2. Pore radius distribution in hardened paste TX (1) and TC (2).

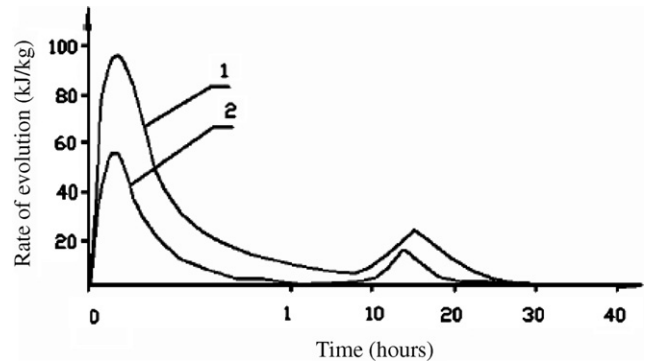


Fig. 3. Heat evolution curves of special slag cement pastes TX (1) and TC (2).

Table 6  
The main-arrays and sub-arrays

Sample	Time-array						
	Y01 (7 d)	Y02 (28 d)	Y1 (0–5 μm)	Y2 (5–10 μm)	Y3 (10–20 μm)	Y4 (20–40 μm)	Y5 (>40 μm)
CSa	26.6	56.2	15.0	12.3	18.2	23.1	31.4
CSb	35.3	70.2	27.3	24.4	24.2	18.6	5.50
CSc	41.0	57.8	43.5	21.7	19.6	12.1	3.10
CSd	35.3	63.0	19.5	13.9	16.0	20.4	30.7
CSe	42.9	67.2	35.1	23.8	19.4	14.2	7.50
CSf	45.8	63.7	46.8	22.2	14.5	10.8	5.70

position. Portland cement was made of 93% clinker and 7% gypsum (percentage by weight) in laboratory mill.

3.2. Experimental program

Slag powder samples which were of different particle size distributions were made by controlling different grinding

time and using two groups of grinders marked as Ma and Mb in laboratory mill. Sample Sa, Sb and Sc were ground by group Ma under duration time 30 min, 80 min and 140 min. Sample Sd, Se and Sf were ground by group Mb under duration time 30 min, 80 min and 140 min. The particle size distribution and the Blaine fineness of the slag powder samples were tested by LS-230 Laser Particle Size

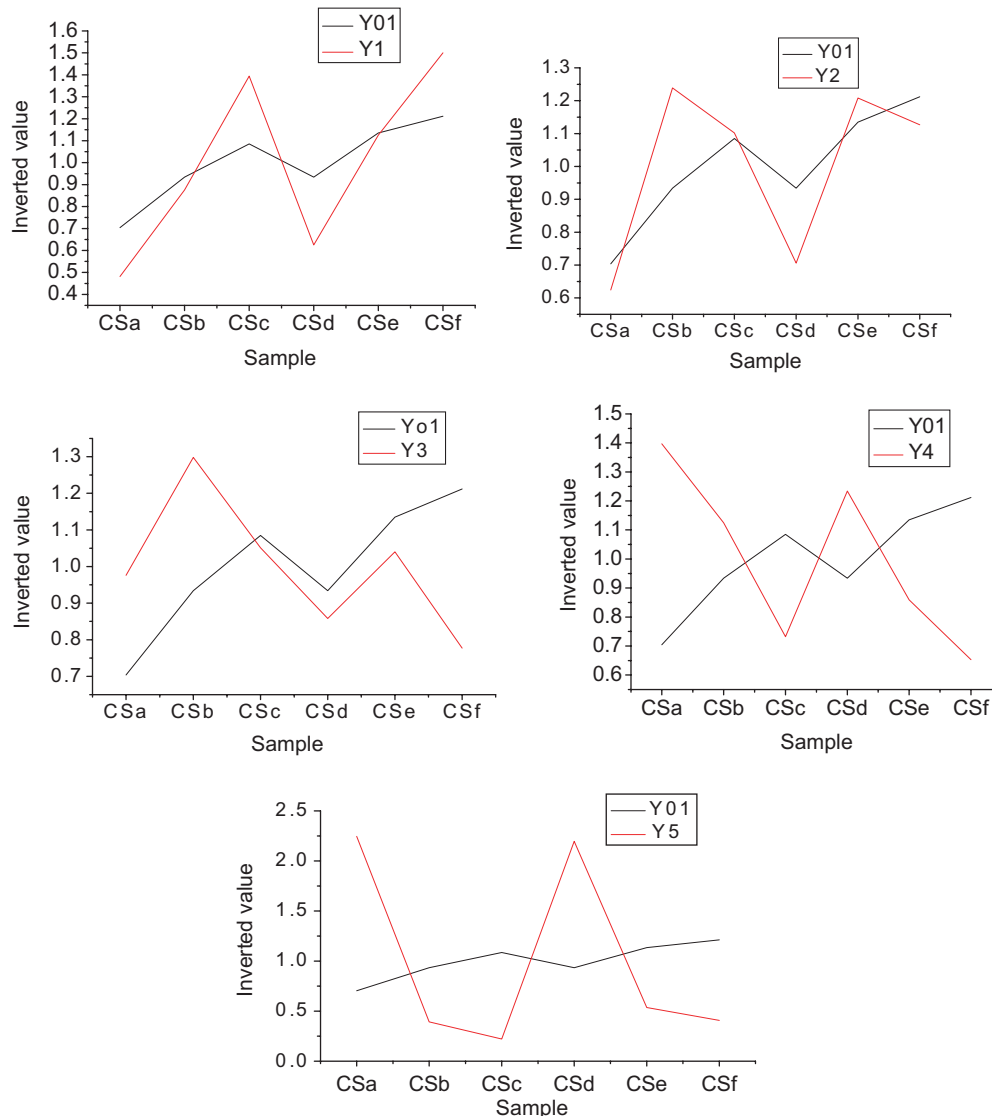


Fig. 4. Main-array and sub-array in pairs Y01–Y1, Y01–Y2, Y01–Y3, Y01–Y4 and Y01–Y5.

Apparatus and Blaine Apparatus separately. The results are shown in Table 2. Slag cements were made of 50% slag powder and 50% Portland cement (percentage by weight). The samples marked as CSa, CSb, etc. were made of 50% slag powder Sa and 50% Portland cement, 50% slag powder Sb and 50% Portland cement, etc. (percentage by weight). According to GB177-85 (Chinese norm), mortar specimens composed of slag cement, standard sand and water in the ratio of 1:2.5:0.44 were made and the mortar compressive strengths at 7 d and 28 d were tested. The compressive strength results are shown in Table 3.

To prove the results of the grey correlation analysis, an air classifier was used to classify slag powder into two size fractions, namely a fine fraction *X* (<20 μm) and a coarse fraction *C* (>20 μm). The particle size distribution of samples *X* and *C* were tested and given in Table 4. The special slag cement samples (TX and TC) were made of 50% *X* or *C* and 50% Portland cement (percentage by weight). The

mortar compressive strength of TX and TC were tested according to GB177-85. The results were shown in Table 5.

The pore structure analysis of hardened slag cement pastes TX and TC were carried out by J5-90 pore structure equipment at the age of 28 d (water-to-solid ratio equal 0.40). The results are given in Fig. 2.

A calorimetric study of special slag cement pastes TX and TC was designed to analyze the reaction between solid and water. The water/solid ratio was 0.45, while the temperature was fixed at 25 °C. The results were given in Fig. 3.

#### 4. Results and discussion

##### 4.1. Qualitative analysis

The mortar compressive strength of slag cement at 7 and 28 d were defined as main-arrays (expressed as Y01 and

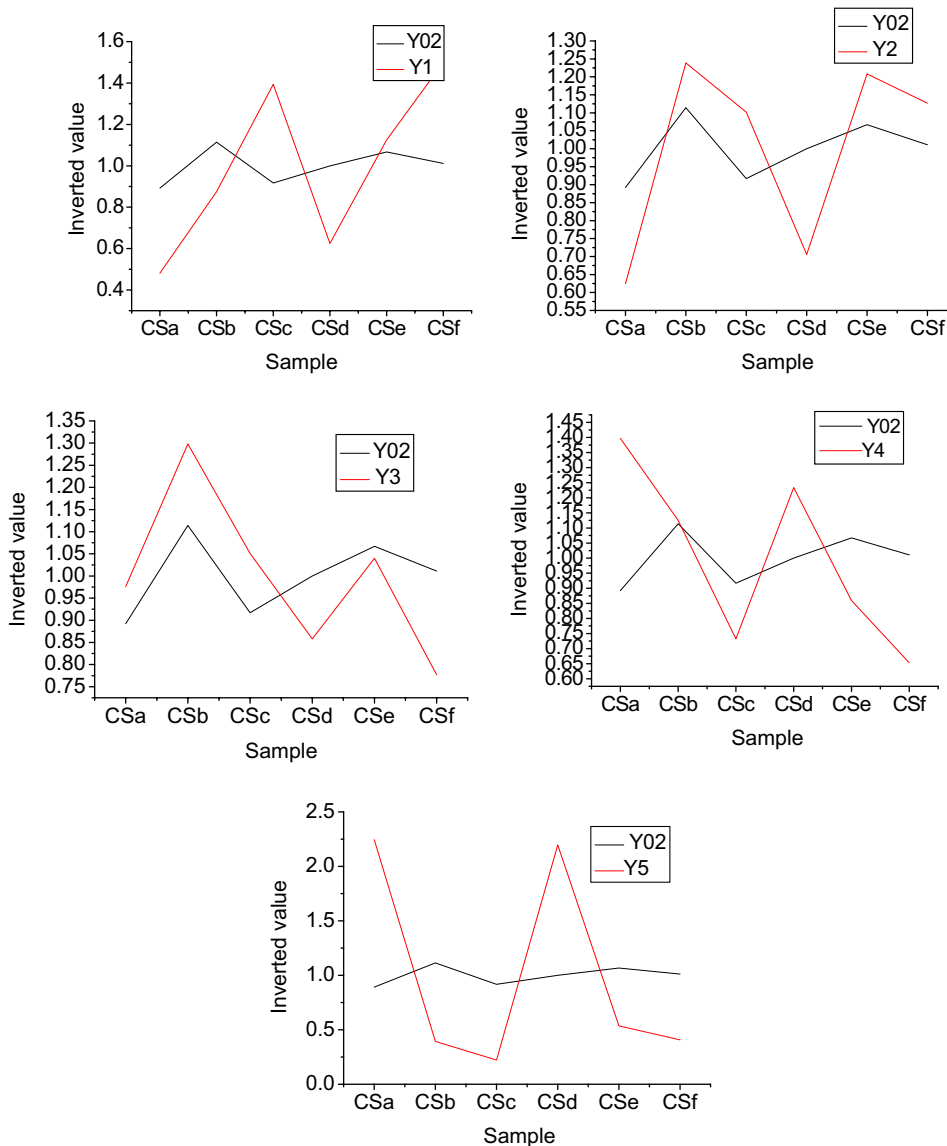


Fig. 5. Main-array and sub-array in pairs Y02–Y1, Y02–Y2, Y02–Y3, Y02–Y4 and Y02–Y05.

Y02) and the volume fractions of particles in different size range of slag powder in slag cement were defined as sub-arrays (expressed as Y1, Y2, etc.). The results are shown in Table 6. The inverted arrays were shown in Figs. 4 and 5. They are graphs of main-array and sub-array in pairs. Fig. 4 shows that the development trend of main-array Y01 was accordant with that of sub-array Y1, Y2 and Y3 (the volume fraction of particles 0–5  $\mu\text{m}$ , 5–10  $\mu\text{m}$  and 10–20  $\mu\text{m}$  of slag powder) well. However, the development trend of main-array Y01 was not similar to that of sub-array Y04 and Y05 (the volume fraction of particles 20–40  $\mu\text{m}$  and >40  $\mu\text{m}$  of slag powder). That means the volume fraction of slag powder 0–20  $\mu\text{m}$  has a positive effect on the mortar compressive strength of slag cement at 7 d while the volume fraction of slag powder >20  $\mu\text{m}$  has a negative effect on it. The results of the relationship between Y02–Y01, Y02–Y02, etc. from Fig. 5 corresponded with those from Fig. 4.

#### 4.2. Grey correlation analysis

The grey correlation degrees were then calculated and shown in Table 7. The results indicated that the volume fraction of particles <20  $\mu\text{m}$  of slag powder had a positive correlation with the mortar compressive strength of slag cement at 7 and 28 d. However, the volume fraction of particles >20  $\mu\text{m}$  of slag powder had a negative correlation with the mortar compressive strength of slag cement at 7 and 28 d. The results were accordant with those of qualitative analysis. The volume fraction of particles 5–10  $\mu\text{m}$  had a maximum effect on the mortar compressive strength of slag cement at 7 d and the volume fraction of particles 10–20  $\mu\text{m}$  had a maximum effect on the mortar compressive strength of slag cement at 28 d. They are key factors.

#### 4.3. Macro and micro-analysis of special slag cement paste

Table 5 shows the results of the mortar compressive strengths of cement TX containing 50% fine slag powder (percentage by weight) and cement TC containing 50% coarse slag powder (percentage by weight). The mortar compressive strengths of cement TX at 7 and 28 d were much higher than those of cement TC.

The results of pore structure analysis (Fig. 2) showed that there are considerable differences in volume of pores at different pore size range in hardened paste with fine slag

powder X and coarse slag powder C. The porosity at different pore size range in hardened paste with fine slag powder X was much less than that in hardened pastes with coarse slag powder C.

Similar situation can be resulted from the heat evolution curves of the cement pastes (Fig. 3). The paste with fine slag powder X indicated a better progress of hydration reaction. The total heat evolved after 40 h of hydration from the paste with fine slag powder X was much more than that from the paste with coarse slag powder C. The tested results consistent with that of macro analysis well.

## 5. Conclusions

The volume fraction of particles 0–20  $\mu\text{m}$  of slag powder had a positive effect on the mortar compressive strength of slag cement at 7 and 28 d while the volume fraction of particles of slag powder larger than 20  $\mu\text{m}$  had a negative effect on it. Among the volume fraction of particles <20  $\mu\text{m}$ , the volume fraction of particles 5–10  $\mu\text{m}$  had a maximum effect on the mortar compressive strength of slag cement at 7 d and the volume fraction of particles 10–20  $\mu\text{m}$  had a maximum effect on the mortar compressive strength of slag cement at 28 d.

## Acknowledgement

The authors gratefully acknowledge the support of 973 National Foundational Research (Number: 2001CB610703).

## References

- [1] Tasdemir C, Tasdemir MA, Lydon FD, Barr BIG. Effects of silica fume and aggregate size on the brittleness of concrete. *Cement Concrete Res* 1996;26(1):63–8.
- [2] Mostafa NY, El-Hemaly SAA, Brown PW. Activity of silica fume and dealuminated kaolin at different temperature. *Cement Concrete Res* 2001;30(6):905–11.
- [3] Li Dongxu, Shen Jinlin, Chen Yimin, Chen Lin, Wu Xuequan. Study of properties on fly ash-slag complex cement. *Cement Concrete Res* 2000;30(9):1381–7.
- [4] Gallias JL, Kara-Ali R, Bigas JP. The effect of fine mineral admixtures on water requirement of cement pastes. *Cement Concrete Res* 2000;30(10):1543–9.
- [5] Li Jianyong, Yao Yan. The research on high property concrete by using super fine slag powder and silica fume. *Concrete* 1997;12(4):12–22.
- [6] Frigione G, Marra S. Relationship between particle size distribution and compressive strength in Portland cement. *Cement Concrete Res* 1976;6(1):113–28.
- [7] Osbaeck B, Johansen V. Particle size distribution and rate of strength development of Portland cement. *J Am Ceram Soc* 1989; 72(2): 197–201.
- [8] Pommersheim JM. Effect of particle size distribution on hydration kinetics. In: Struble LJ, Brown PW., editors. *Materials research society symposium proceedings*, 85, Mat Res Soc, 1987, Pittsburgh, p. 301–6.
- [9] Knudsen T. The dispersion model for hydration of Portland cement, general concepts. *Cement Concrete Res* 1984;14:622–30.

Table 7  
Grey correlation degree

Main-array (compressive strength)	Sub-array				
	Y1	Y2	Y3	Y4	Y5
Age (d)	(0–5 $\mu\text{m}$ )	(5–10 $\mu\text{m}$ )	(10–20 $\mu\text{m}$ )	(20–40 $\mu\text{m}$ )	(>40 $\mu\text{m}$ )
Y01 (7)	+0.8184	+0.8757	+0.6628	–0.6838	–0.4769
Y02 (28)	+0.6933	+0.8002	+0.8540	–0.7629	–0.4678

- [10] Wakasugi S, Sakai K, Shimobayashi S, Watanabe H. Properties of concrete using belite-based cement with different fineness. In: Gjorv OE, editor. *Concrete under severe conditions*, vol. 2. London: E and FN Spon; 1998. p. 2161–9.
- [11] Taylor HFW. *Cement Chemistry*. 2nd ed. London: Thomas Telford; 1997.
- [12] Bentz DP, Garboczi EJ, Haecker CJ, Jensen OM. Effects of cement particle size distribution on performance properties of Portland cement-based materials. *Cement Concrete Res* 1999; 29:1663–71.
- [13] Ranganath RV, Bhattacharjee B, Krishnamoorthy S. Influence of size fraction of ponded ash on its pozzolanic activity. *Cement Concrete Res* 1998;28:749–61.
- [14] Olorunsogo FT. Particle size distribution of ggbs and bleeding characteristics of slag cement mortar. *Cement Concrete Res* 1998;28(6):907–19.
- [15] Grzeszczyk S, Lipowski G. Effect of concrete and particle size distribution of high-calcium fly ash on the rheological properties of cement pastes. *Cement Concrete Res* 1997;27(6):907–16.
- [16] Mehta PK. Influence of the fly ash characteristics on the strength of Portland-fly ash cement. *Cement Concrete Res* 1985;15(4): 669–73.
- [17] Deng J. *Grey control system*. Wuhang, China: Huazhong Engineering College Press; 1985.
- [18] Patton MQ. *Qualitative evaluation and research methods*. Calif.:Sage Publications; 1990.